Beam Research Program

Lawrence Livermore National Laboratory

Research Mer

Title: Phase Compensated Fine Scale Thermal Blooming

Author(s): John J. Barnard

RM 89-10

Date March 7, 1989

No. pages 18

Summary:

We derive the growth rates for the fine scale thermal blooming instability in a phase compensated, high power laser beam. This work extends the work of previous authors to include the effects of single short laser pulses and the effects of windshear.

CLASSIFIED BY: [signature] 3-8-89

UNCLASSIFIED

Category

- ■ Theory Computations
- ☐ Experiment
- ☐ Electrical Engineering
- ☐ Mechanical Engineering
- ☐ Diagnostics
- ☐
- ☐

- ☐ ELF
- ☐ PALADIN
- ☐ AIRLINE I
- ☐ AIRLINE II
- ☐
- ☐

- ☐ CPB
- ■ FEL
- ☐ Accelerator
- ☐
- ☐

- ☐ ATA Note
- ☐ Beam Physics
- ☐ ELF Note
- ☐ PALADIN Paper
- ☐
- ☐

- ☐ ETA
- ☐ ATA
- ☐ ETA II
- ☐ ALEX
- ☐
- ☐

Distribution

- ■ Beam Research
- ■ Physics
- ☐ Electrical Engineering
- ☐ Mechanical Engineering
- ☐ Diagnostics
- ☐ List
- ☐ Internal Distribution Only
- ☐
- ☐

Phase Compensated Fine Scale Thermal Blooming

John J. Barnard
Lawrence Livermore National Laboratory, University of California
P.O. Box 808, L626, Livermore, California 94550

Abstract

We derive the growth rates for the fine scale thermal blooming instability in a phase compensated, high power laser beam. This work extends the work of previous authors to include the effects of single short laser pulses and the effects of windshear.

I. INTRODUCTION

The fine-scale thermal blooming instability has been investigated computationally (Refs. 1,2, and 3) and analytically (Refs. 4 - 11, 15). The computational work resulted in the discovery of the instability and continues to provide the most accurate description of a real beam propagating through a real atmosphere. The analytical results, however, provide a way of understanding the physics of this instability under simplified assumptions, allowing some physical insight into the instability that can be more difficult to glean from the numerical results alone. This note analytically treats the phase compensated instability (and thus augments previous work by the author in ref. 9, which dealt with an uncompensated beam), but includes the effects of short pulse times and wind shear (and thus generalizes somewhat the work of reference 4). As in reference 9, the main purpose of this work will be to obtain the scaling laws for the growth rate, as a function of pulse time and perturbation wavelength. As I will be relying heavily on references 4 and 9, equations from those references will be referred to as, for example, 4-3 denoting equation (3) from reference 4.

II. GENERALIZED PROPAGATION EQUATIONS

As in reference 4, we let I_1 and S_1 be the intensity and phase perturbation upon a uniform beam of intensity I_o, and phase S_o. The index of refraction perturbation is denoted n_1, and the intensity and phase perturbation of the "beacon" as described in reference 4, will be denoted I_{1B} and S_{1B}, whereas the unperturbed beacon intensity are given by I_{oB} and S_{oB}. Finally the normalized beacon intensity perturbation is defined as $\psi_B = I_{1B}/I_{oB}$. The intensity and phase equations (eqs. 4-10, 4-11, 4-48, and 4-49) for both the beacon and beam are Fourier transformed in x and y, extracting the fourier component with perturbation wave number $\underline{k}_\perp$. The resulting equations are Laplace transformed in time, with hats indicating the transformed variables. Upon elimination of the beam and beacon phase, equations 9-23 and 4-52 are obtained:

$$\frac{\partial^2 \hat{I}_1}{\partial z^2} + \frac{k_\perp^4}{4k^2}\hat{I}_1 = \frac{I_o k_\perp^2}{n_o}\hat{n}_1 \qquad (1)$$

$$\frac{\partial^2 \hat{\psi}_B}{\partial z^2} + \frac{k_\perp^4}{4k^2}\hat{\psi}_B = \frac{k_\perp^2}{n_o}\hat{n}_1 \tag{2}$$

We assume (as in references [4] and [9]), that the index of refraction is only a function of density. Thus,

$$\hat{n}_1 = \frac{dn}{d\rho}\hat{\rho}_1 \tag{3}$$

The density perturbations arise from the absorption of beam energy, and conversion into thermal energy. This is described by the fluid equations [eqs (9-1) to (9-3)]. As in equation (9-34) we may express the index of refraction perturbations as a function of intensity perturbation, and the state of the atmosphere at $t = 0$:

$$\hat{n}_1 = -f\hat{I}_1 + g \tag{4}$$

Here $f = \gamma\Gamma(\underline{M}^{-1})_{14}$ and $g = \rho_o(dn/d\rho)\underline{M}_{1i}^{-1}\underline{C}_{oi}$ where $\underline{M}$ is defined in equation (9-30), and $\underline{C}_{oi}$ is defined in equation (9-31) and Γ is defined following (9-35). (Note that in ref. 9, $\underline{M}$ has been Laplace transformed in t and z; here we do not transform in z). In the limit of large t analyzed in reference (4) (in which thermal diffusion was ignored):

$$f = \frac{\Gamma}{s + i\underline{k}_\perp \cdot \underline{v}} \tag{5}$$

$$g = \frac{n_1(t=0;z)}{s + i\underline{k}_\perp \cdot \underline{v}} \tag{6}$$

In reference 4, f was considered constant with respect to z and g was assumed to be proportional to $\delta(z-h)$ where h is the height of a uniform atmosphere. Wind shear may be included by allowing $\underline{k}_\perp \cdot \underline{v}$ to be a function of z, and so both f and g will be functions of z.

A general evaluation of $(\underline{M}^{-1})_{14}$ yields:

$$f = \frac{\Gamma c_s^2 k_\perp^2}{s_o(s_o + \gamma\chi k_\perp^2)(s_o + [\nu+\theta]k_\perp^2) + c_s^2 k_\perp^2(s_o + \chi k_\perp^2)} \tag{7}$$

Here the notation is as in ref. 9: c_s is the sound speed, $s_o = s + i\underline{k}_\perp \cdot \underline{v}$, γ is the ratio of specific heats, χ is the diffusion coefficient, ν and θ are viscosity coefficients defined after eq. 9-27. In general g is a function of velocity, density and temperature perturbations, all of which can be functions of z. If pulse times are short (i.e. if $c_s k_\perp \ll |s_o|$) and if diffusion and viscosity can be ignored equation (7) is approximately given by:

$$f \cong \Gamma c_s^2 k_\perp^2 / s_o^3 \tag{8}$$

As discussed in ref. 9, following eq. 9.62, s_o may be regarded as constant with respect to z when $c_s k_\perp \ll |s_o|$.

Substituting eq. (4) into equations (1) and (2) yields:

$$\frac{\partial^2 \hat{I}_1}{\partial z^2} + \left(\frac{k_\perp^4}{4k^2} + \frac{f k_\perp^2 I_o}{n_o}\right)\hat{I}_1 = \frac{I_o k_\perp^2 g}{n_o} \tag{9}$$

$$\frac{\partial^2 \hat{\psi}_B}{\partial z^2} + \frac{k_\perp^4}{4k^2}\hat{\psi}_B = \frac{-k_\perp^2 f}{n_o}\hat{I}_1 + \frac{k_\perp^2 g}{n_o} \tag{10}$$

As in reference (4) equation (9) is solved generally, with arbitrary $\hat{I}_1(z=0)$ and $\frac{\partial \hat{I}_1(z=0)}{\partial z}$. This general solution is substituted into equation (10), with the boundary condition on ψ_B at $z = h$ that:

$$\hat{\psi}_B(z=h) = 0 \quad \text{and} \quad \frac{\partial \hat{\psi}_B(z=h)}{\partial z} = 0. \tag{11}$$

The beacon intensity is then expressable in terms of the beam intensity and phase at $z = 0$. The feedback condition for phase compensation,

$$\frac{\partial \hat{\psi}(z=0)}{\partial z} = \frac{1}{I_o}\frac{\partial \hat{I}_1(z=0)}{\partial z} \tag{12}$$

The form of of eq. 9 suggests that we define k_z by:

$$k_z^2 = k_f^2 + \frac{f k_\perp^2 I_o}{n_o} \tag{13}$$

Here $k_f = k_\perp^2/2k$.

If k_z is constant with respect to z the general solution to eq. (9) is:

$$\hat{I}_1(z) = \hat{I}_1(z=0)\cos k_z z + \frac{k_\perp^2 I_o}{k_z}\hat{S}_1(z=0)\sin k_z z + \frac{k_\perp^2 I_o}{n_o k_z}\int_0^z dz' g(z')\sin k_z(z-z'). \tag{14}$$

Here $S_1(z=0) = (I_o k_\perp^2)^{-1}(\frac{\partial \hat{I}_1(z=0)}{\partial z})$.

If k_z is not a constant, but varies slowly enough such that $dk_z/dz \ll k_z^2$, the WKB approximation (see e.g. ref. 12) may be used to solve eq. (9). The WKB generalization of eq. (14) is:

$$\hat{I}_1(z) \cong \left(\frac{k_{zo}}{k_z}\right)^{1/2}\Bigg[\hat{I}_1(z=0)\cos\int_0^z dz' k_z(z')$$

$$+\left(\frac{k_\perp^2 I_o}{k_{zo}}\hat{S}_1(z=0) + \frac{k'_{zo}}{k_{zo}^2}\hat{I}_1(z=0)\right)\sin\int_0^z dz' k_z(z')\Bigg] +$$

$$+\frac{I_o k_\perp^2}{n_o k_{zo}}\int_0^z dz'\left(\frac{k_{zo}^2}{k_z(z)k_z(z')}\right)^{1/2} g(z')\sin\int_{z'}^z dz'' k_z(z'') \tag{15}$$

Here $k_{zo} = k_z(z=0)$ and $k'_{zo} = dk_z/dz$ at $z = 0$.

Although a more general feedback condition than eq. (12) may be used we restrict our attention to strict phase compensation, so we assume that $\hat{I}_1(z=0)=0$. The general solution to equation (10) subject to the boundary conditions in eq. (11) is:

$$\psi_B = \frac{1}{k_f}\int_z^h dz' m(z') \sin k_f(z'-z) \tag{16}$$

where

$$m(z) = \frac{-k_\perp^2 f}{n_o}\hat{I}_1(z) + \frac{k_\perp^2 g(z)}{n_o}.$$

Substituting eq. (14) into eq. (16) yields:

$$\hat{\psi}_B = \frac{k_\perp^2 \hat{S}_1(z=0)}{k_z}[\sin k_z z - \sin k_z h \cos k_f(h-z) + \frac{k_z}{k_f}\cos k_z h \sin k_f h \sin k_f(h-z)] +$$

$$\frac{k_\perp^2}{n_o k_f}\int_z^h dz' g(z') \sin k_f(z'-z) - \frac{k_\perp^4 I_o f}{n_o^2 k_z k_f}\int_z^h dz' \sin k_f(z'-z)\int_0^{z'} dz'' g(z'') \sin k_z(z'-z'') \tag{17}$$

If eq. (15) is substituted into eq. (16) instead, we obtain the WKB generalization of eq. (17):

$$\hat{\psi}_B = \frac{-k_\perp^4 I_o}{n_o k_f k_{zo}}\hat{S}_1(z=0)\int_z^h dz' f(z') \sin k_f(z'-z) \sin \int_0^{z'} dz'' k_z(z'') +$$

$$+\frac{k_\perp^2}{n_o k_f}\int_z^h dz' g(z') \sin k_f(z'-z)$$

$$\frac{k_\perp^4 I_o}{n_o^2 k_f k_{zo}}\int_z^h dz' f(z') \sin k_f(z'-z)\int_0^{z'} d\xi \left(\frac{k_{zo}^2}{k_z(z')k_z(\xi)}\right)^{1/2} g(\xi) \sin \int_\xi^{z'} dz'' k_z(z'') \tag{18}$$

Imposing the feedback condition, eq. (12), we obtain

$$\hat{S}_1(z=0) = -\frac{n(s)}{d(s)} \tag{19}$$

where

$$n(s) = \frac{1}{n_o}\int_0^h dz' g(z') \cos k_f z'$$

$$-\frac{k_\perp^2}{n_o^2 k_{zo}}\int_0^h dz' f(z') \cos k_f z' \int_0^{z'} d\xi \left(\frac{k_{zo}^2}{k_z(z')k_z(\xi)}\right)^{1/2} g(\xi) \sin \int_\xi^{z'} dz'' k_z(z'') \tag{20}$$

and

$$d(s) = 1 - \frac{k_\perp^2 I_o}{n_o k_{zo}} \int_0^h dz' f(z') \cos k_f z' \sin \int_0^{z'} dz'' k_z(z'') \tag{21}$$

Substituting eq. (19) into eq. (15), and evaluating at $z = h$, where h is the propagation path length yields:

$$\hat{I}_1(h,s) = \frac{I_o k_\perp^2}{d(s)} \left[\frac{-Gn(s)}{[k_{zo} k_z(h)]^{1/2}} \sin \int_0^h dz' k_z(z') + \right.$$

$$\left. + \frac{d(s)}{n_o} \int_0^h dz' \frac{g(z')}{[k_z(h) k_z(z')]^{1/2}} \sin \int_{z'}^h dz'' k_z(z'') \right] \tag{22}$$

The Laplace inversion of eq. (22) is:

$$I_1(h,t) = \frac{1}{2\pi i} \int_{C-i\infty}^{C+i\infty} \hat{I}_1(h,s) \exp(st) ds. \tag{23}$$

Equation 23 may be evaluated by the method of residues. Thus eq. (23) is solved by solving the equation

$$d(s) = 0. \tag{24}$$

The solution to equation (23) will asymptotically satisfy $I_1(h,t) \sim \exp st$ where s is the solution to equation (24) with the largest positive real part.

III. CONSTANT k_z

For the case that f and thus k_z are constant with respect to z we (not surprisingly) obtain the result 4-64:

$$\cos k_z h \cos k_f h + \frac{k_f}{k_z} \sin k_z h \sin k_f h = 0 \tag{25}$$

As found in ref. (4) if $|k_f| << |k_z|$ equation (25) becomes

$$\cos k_z h \cong 0 \quad \Rightarrow \quad \left(\frac{f k_\perp^2 I_o}{n_o} \right)^{1/2} h = (2n+1) \frac{\pi}{2} \tag{26}$$

In the large time limit (i.e. $|s_o| \ll c_s k_\perp$) we approximate eq. (7) and recover the result of ref. 4 (cf. eq. 4-62; here diffusion has been included, as well):

$$s_o t = \frac{4\Gamma I_o k_\perp^2 h^2 t}{\pi^2 (2n+1)^2 n_o} - \chi k_\perp^2 t = \frac{8}{\pi^2 (2n+1)^2} N_D \kappa^2 - x\kappa^2 \tau \qquad (c_s k_\perp \gg |s_o|) \tag{27}$$

Here $N_D = \Gamma I_o k h t / n_o$, $\kappa = (h/2k)^{1/2} k_\perp$, $\tau = (2k/h)^{1/2} c_s t$, and $x = (2k/h)^{1/2} \chi / c_s$.

In the small time limit, eq. (8) may be combined with eq. (26) to give:

$$s_o t = \left(\frac{4\Gamma I_o c_s^2 k_\perp^4 h^2 t^3}{(2n+1)^2 \pi^2 n_o} \right)^{1/3} = \left(\frac{8}{(2n+1)^2 \pi^2} N_D \kappa^4 \tau^2 \right)^{1/3} \qquad (c_s k_\perp \ll |s_o|) \tag{28}$$

In the limit that diffraction becomes important, then $|k_f| \cong |k_z|$ and equation (25) becomes:

$$\cos(k_z - k_f)h \cong 0 \quad \Rightarrow \quad \frac{fk_\perp^2 I_o h}{2k_f n_o} \cong (2n+1)\frac{\pi}{2} \tag{29}$$

Thus in the limits of short and long time the quantity $s_o t$ can be written:

$$s_o t \cong \begin{cases} \frac{2\Gamma I_o kht}{\pi(2n+1)} = \frac{2N_D}{\pi(2n+1)} & c_s k_\perp \gg |s_o| \\ \left(\frac{2\Gamma I_o khc_s^2 k_\perp^2 t^3}{\pi(2n+1)n_o}\right)^{1/3} = \left(\frac{2N_D \kappa^2 \tau^2}{\pi(2n+1)}\right)^{1/3} & c_s k_\perp \ll |s_o| \end{cases} \tag{30}$$

Thus, as in the uncompensated case, the phase compensated instability gain is reduced when the sound travel time across a perturbation is large compared to the growth time.

IV. WIND SHEAR (VARIABLE k_z)

In order to treat the case of a wind which is non-uniform in z, we return to eq. (21) and make the assumption that:

$$\underline{k}_\perp \cdot \underline{v}(z) = \underline{k}_\perp \cdot \underline{v}_o + k_\perp v' z$$

Again we split the problem into the two regimes when diffraction is and is not important. Equation (13) can be approximated in the two regimes:

$$k_z \cong \begin{cases} k_f + \frac{\Gamma I_o k}{n_o(s_o + ik_\perp v' z)} & \text{if } k_f^2 \gg \left|\frac{\Gamma I_o k_\perp^2}{n_o(s_o + ik_\perp v' z)}\right| \\ \left(\frac{\Gamma I_o k_\perp^2}{n_o(s_o + ik_\perp v' z)}\right)^{1/2} & \text{if } k_f^2 \ll \left|\frac{\Gamma I_o k_\perp^2}{n_o(s_o + ik_\perp v' z)}\right| \end{cases} \tag{31}$$

Here and subsequently $s_o = s + i\underline{k}_\perp \cdot \underline{v} =$ a constant with respect to z. Using the upper of eq. (31), we may approximate eqns. (21) and (24) in the small k_f (negligible diffraction) limit by:

$$1 - \frac{\Gamma I_o k_\perp^2}{n_o k_{zo}} \int_0^z \frac{dz'}{s_o + ik_\perp v' z'} \sin \frac{2(\Gamma I_o)^{1/2}}{iv' n_o^{1/2}} [(s_o + ik_\perp v' z)^{1/2} - s_o^{1/2}] = 0 \tag{32}$$

We may introduce two variables with the dimensions of frequency:

$$s_D = \Gamma I_o kh/n_o \quad \text{and} \quad s_w = ik_\perp v' h$$

Also the following dimensionless variables are of use,

$$a = 2\left(\frac{-\Gamma I_o s_o}{n_o v'^2}\right)^{1/2} = \left(\frac{8 s_o s_D k_f h}{s_w^2}\right)^{1/2}; \qquad b = -i\left(\frac{\Gamma I_o k_\perp h}{n_o v'}\right) = \left(\frac{2 s_D k_f h}{s_w}\right),$$

and

$$a_1 = a(1 + \frac{4b}{a^2})^{1/2} = a(1 + \frac{s_w}{s_o})^{1/2}.$$

We may then transform eq. (32) to:

$$0 = 1 - a\int_0^{a_1 - a} dx \frac{\sin x}{x + a} \tag{33}$$

The integration may be expressed in terms of the cosine- and sine-integrals (cf. e.g. ref. 13):

$$0 = 1 - a\big(\cos a[\mathrm{si}(a_1) - \mathrm{si}(a)] - \sin a[\mathrm{ci}(a_1) - \mathrm{ci}(a)]\big). \tag{34}$$

Here

$$\mathrm{si}(x) = -\int_x^\infty dx \frac{\sin x}{x} \quad \text{and} \quad \mathrm{ci}(x) = -\int_x^\infty dx \frac{\cos x}{x}. \tag{35}$$

If $|a|$ and $|a_1|$ are much greater than unity asymptotic expressions for $\mathrm{si}(x)$ and $\mathrm{ci}(x)$ may be used:

$$\mathrm{si}(x) \cong \frac{-\cos x}{x} \quad \text{and} \quad \mathrm{ci}(x) \cong \frac{\sin x}{x} \qquad (x \gg 1). \tag{36}$$

Substituting eq. (36) into eq. (34) yields:

$$\cos(a_1 - a) = 0 \quad \Rightarrow \quad a_1 - a = (2n+1)\frac{\pi}{2}. \tag{37}$$

Solving eq. (37) for s_o yields:

$$s_o = \frac{4\Gamma I_o k_\perp^2 h^2}{(2n+1)^2\pi^2 n_o} - \frac{(2n+1)^2\pi^2 n_o v'^2}{64\Gamma I_o} - \frac{iv' k_\perp h}{2}. \tag{38}$$

The assumption that $|a|$ and $|a_1|$ be much greater than unity, can be shown to be approximately equivalent to assuming that either $|s_w| \ll s_D(k_f h)^2$ or that $n \gg 1$. It is apparent from eq. (38) that small amounts of wind shear will lower the growth rate and will be most noticeable at small values of $k_\perp$.

In the large $k_\perp$ limit, when the lower of eqs. (31) is substituted into eq. (21), we obtain:

$$0 = 1 - \frac{2s_D k_f h}{s_o k_f h + s_D}\int_0^1 \frac{dx}{(1 + \frac{s_w}{s_o}x)} \cos k_f h x \sin\big(k_f h x + \frac{s_D}{s_w}\ln(1 + \frac{s_w}{s_o}x)\big) \tag{39}$$

Here the integration variable $x = z/h$.

Expanding the sin in eq. (39) and evaluating part of the integral:

$$0 = 1 - \frac{s_D k_f h}{s_o k_f h + s_D}\Bigg[\frac{s_o}{s_D}\Big(1 - \cos\big(\frac{s_D}{s_w}\ln(1 + \frac{s_w}{s_o})\big)\Big) + \\ + \int_0^1 \frac{dx}{(1 + \frac{s_w}{s_o}x)} \sin\big(2k_f h x + \frac{s_D}{s_w}\ln(1 + \frac{s_w}{s_D}x)\big)\Bigg]. \tag{40}$$

The final integral is of order $(k_f h)^{-1}$ whereas the remaining terms in the large brackets are of order unity. Thus in the large $k_f h$ limit eq. (40)becomes:

$$0 \cong \cos\left(\frac{s_D}{s_w}\ln(1+\frac{s_w}{s_o})\right) \quad \Rightarrow \quad s_o \cong \frac{s_w}{\exp\left((2n+1)\frac{\pi}{2}\frac{s_w}{s_D}\right)-1}. \tag{41}$$

Separating the real and imaginary parts of eq. (41) yields:

$$\frac{s_o}{|s_w|} = -\frac{i}{2} + \frac{1}{2}\left[\frac{\sin x_n}{1-\cos x_n}\right] \qquad x_n = (2n+1)\frac{\pi}{2}\frac{|s_w|}{s_D} \tag{42}$$

When $x_n \ll 1$

$$s_o = \frac{2}{(2n+1)\pi}\frac{\Gamma I_o k h}{n_o} - \frac{(2n+1)\pi}{24}\frac{k_\perp^2 v'^2 h n_o}{\Gamma I_o k} - \frac{i k_\perp v' h}{2} \tag{43}$$

In order to perform the integration in eq. (23) some care must be taken when summing the residues at the poles in eqs. (41) and (42). The integral in equation (23) can be written:

$$I(h,t) = \frac{1}{2\pi i}\int_{C-i\infty}^{C+i\infty} \frac{F(s_o)e^{s_o t}ds_o}{\cos\left(\frac{s_D}{s_w}\ln(1+\frac{s_w}{s_o})\right)} \tag{44}$$

Here $F(s_o)$ depends on $g(z,s_o)$ which in turn depends on the initial index perturbation $n_1(t=0;z)$(*cf.* eqs. [20] through [22]). Physical distributions should not result in poles in $F(s_o)$ with positive real s_o. In order to keep the logarithm in eq. (43) single valued a branch cut is required with endpoints on the singularities in the logarithm at $s_o = 0$ and $s_o = -i|s_w|$ (see figure [1]). We choose the branch cut which connects the two singularities, and choose the branch of the logarithm such that:

$$-\pi \le \arg(1+\frac{s_w}{s_o}) \le \pi \tag{45}$$

The poles in eq. (41) or (42) all occur somewhere along the line $\mathrm{Im}(s_o) = -|s_w|/2$. However not all integers n correspond to solutions on this branch of the logarithm. Eq. (45) and (41) imply that n must satisfy:

$$|(2n+1)\frac{\pi}{2}| < \pi\frac{s_D}{|s_w|} \tag{46}$$

We thus obtain contributions to the integral in equation (44) from the poles satisfying both eqs. (46) and (42), and a counter-clockwise integration around the branch cut. Examination of the integrand in the branch cut integration, reveals a function which is well behaved, though difficult to analytically integrate. Since $\mathrm{Re}(s_o) \to 0$ in the branch cut integration, the branch cut contributes a part of the solution which oscillates but does not grow in time. The dominant growing mode is thus approximately given by eq. (43) with $n = 0$, for $s_D/|s_w| > \pi$, and with only oscillations present for $s_D/|s_w| < \pi$. Thus

wind shear lowers the growth rate at large values of $k_\perp$. Physically eqs. (38) and (43) can be interpreted as follows. The growth times τ_G in the large and small $k_\perp$ regimes in the absence of wind shear are: $\tau_G \sim 1/(s_D k_f h)$ (for small $k_\perp$) and $\tau_G \sim 1/s_D$ (for large $k_\perp$). The wind shearing time for the perturbation, $\tau_w \sim 2\pi/(k_\perp v' h)$. So in the large $k_\perp$ regime, the wind shearing time is shorter than the growth time *above* a critical $k_\perp$, (where $\tau_G \sim \tau_w$)and in the small $k_\perp$ regime the wind shearing time is shorter than the growth time *below* a critical $k_\perp$ (where again $\tau_G \sim \tau_w$). Equations (38) and (43) indicate that when $\tau_G > \tau_w$ the perturbations do not grow.

The previous discussion used a specific form for the wind shear, i.e. a wind having a linear gradient in z. To what extent do the results depend on this form for the shear? To answer that question, we may rewrite eq.(21) (for which only the WKB assumption $[|dk_z/dz| << |k_z|^2]$ has been made):

$$d(s) = 1 - \frac{1}{k_{zo}} \int_0^h dz' [k_z^2(z') - k_f^2] \cos k_f z' \sin \bar{k}_z(z') z' \tag{47}$$

Here

$$\bar{k}_z(z) = \frac{1}{z} \int_0^z dz \; k_z(z). \tag{48}$$

Straightforward algebra leads to the following approximate forms for the dispersion relation d(s)=0:

$$0 = d(s) \cong \begin{cases} \cos[(\bar{k}_z(h) - k_f)h] & \text{if } |k_z| \cong k_f \gg |k_z - k_f| \\ 1 - \frac{1}{k_{zo}} \int_0^h dz \; k_z^2(z) \sin \bar{k}_z z & \text{if } |k_z| \gg k_f \\ \cos \bar{k}_z(h) h & \text{if } |k_z| \gg k_f \text{ and } |k_z| \cong |k_{zo}| \end{cases} \tag{49}$$

Equations (41),(34), and (37) represent, respectively, the top, middle, and bottom of equations (49) for the case of a linear gradient in the wind, while equations (29) and (26) are the respective reduction of the top and bottom equations for the case of no wind shear.

V. DISCUSSION AND CONCLUSION

Note that we have assumed that

$$\underline{k}_\perp \cdot \underline{v} = \underline{k}_\perp \cdot \underline{v}_o + k_\perp v' z = \underline{k}_\perp \cdot \underline{v}_o + \underline{k}_\perp \cdot \frac{d\underline{v}}{dz} z.$$

Since $d\underline{v}/dz$ is not necessarily aligned with $\underline{v}_o$, we may write $v' = |d\underline{v}/dz| \cos\phi$, where ϕ is the angle between the shearing direction and the perturbation wavevector $\underline{k}_\perp$. As pointed out in ref. (6) when $\phi = \pi/2$ the growth of the perturbation wavevector is not affected by the shear, whereas when $\phi = 0$ the shear is most able to mix different phases of the perturbation at different altitudes, thus lowering the growth rate.

Figure 2 outlines the borders of the asymptotic regimes described by equations (27), (28), (30), (38) and (43) in the $k_\perp - t$ plane, with the distortion number N_D (or equivalently the energy per pulse) held constant. The real part of the growth rate of the fastest growing mode times the pulse time (i.e. the logarithm of the gain) is indicated in the region where

it is valid. A few contours of G, the logarithmic gain, are shown. Figure 3 is a surface plot of G as a function of the same parameters. Here, G has been artificially smoothed by inverting the sum of the inverse growth rates and summing the decay rates found in each asymptotic region. In figures 2 and 3, $\phi = \pi/2$. Figures 4 and 5, are the corresponding figures with $\phi = 0$, and $|d\underline{v}/dz| = v_o/h$. $N_D = 1000$ has been assumed in figures 2 through 5.

The dotted lines in figures 2 and 4 indicate roughly where current technology limits the application of the boundary condition (eq. 12). That is, we expect that the actuators which control the phase front on a beam director of several meters, will not likely be spaced closer than ~1 cm, while actuator time response is not likely to be much faster than $\sim 10^3 s^{-1}$. For perturbation wavelengths and pulse times less than these respective cutoffs, growth will occur at a smaller rate but no less than the free beam growth rates of ref. 9. (In ref. 3, it was found that non-linear coupling of the low-wavenumber instability, produces growth at high wavenumber beyond the actuator cutoff).

As can be seen from figures 2 through 5 single short pulses ($\Delta t \sim 10^{-3}$ to $\sim 10^{-1}$s for $N_D = 1000$) will have somewhat smaller instability gains due to acoustic effects. Wind shear has virtually no effect on short pulses (cf. ref. 9). At large times however wind shear can substantially reduce the gain for $\phi < \pi/2$. Figure 6 illustrates the gain for a 1 s pulse as a function of $|\underline{k}_\perp|$ and ϕ with $N_D = 150$. (The 'smoothed' gain has again been used.) It is apparent that there is a critical angle ϕ_c at which the logarithmic gain goes to zero. By simultaneously solving for $G = 0$ and $dG/dk_\perp = 0$ we obtain:

$$\cos\phi_c \cong 1.3\frac{N_D}{\beta\tau} \tag{50}$$

Here,

$$\beta = \frac{h}{c_s}\left|\frac{d\underline{v}}{dz}\right|.$$

It is apparent that if $N_D/\beta\tau <\sim .8$ there will be no growth of perturbations at $\phi = 0$ and that as $N_D/\beta\tau$ approaches zero the angular extent of growing perturbations goes to zero. We conclude that if $N_D > 1$,

$$N_D/\beta\tau << 1 \tag{51}$$

is necessary for maintenance of a collimated beam. (This condition may not be sufficient, however, if the small range in angle of unstable wavevectors is made up for by the large amplitude of the growing mode at $\phi = \pi/2$. In a real atmosphere if $|\pi/2 - \phi_c|$ is less than the angular dispersion of the wind direction when averaged over a pulse time, we expect that beam degradation will be minimal.) Atmospheric turbulence will also act to stabilize the perturbations, again shearing the perturbations over large eddy lengths. $|d\underline{v}/dz|$ should then be replaced by $v_t(\ell)/\ell$ in eq. (51) where v_t is the turbulent velocity associated with the largest scale ℓ of the turbulence. (Note that the quantity S used in ref. 3 to characterize their numerical results is defined as $S = (\Delta v/v_o)(N_F/N_\lambda)$, where $\Delta v = h\ dv/dz$, $N_\lambda = (N_D/2\pi)(D/v_o t)$, $N_F = kD^2/(4h)$, and D = the diameter of the laser beam. Thus $N_D/\beta\tau = \pi/[2^{1/2}S]$.)

Thus, the need to compensate for the inhomogeneous and fluctuating index of refraction in the atmosphere has resulted in the idea of phase compensation of a trans-atmospheric laser beam. However, the realization that at high power these beams will have the property that fine scale thermal inhomogeneities rapidly grow and degrade the beam, has motivated the conception of more sophisticated compensation schemes such as conjugate laser heating (ref. 14) or field (intensity and phase) conjugation (e.g. refs. 3, 15). If phase conjugation alone is used eq. 51 indicates that wind shear allows for somewhat less stringent limits than without shear. For example, a modest shear of 450 cm s^{-1} (10 mph) over 5 km ($\beta = .015$), with a laser wavelength of 1μ, and a pulse length of 1 s ($\tau \cong 1.5 \times 10^4$) requires the distortion number to be less than $\sim$200. For a 10 m beam director, and an atmospheric absorption coefficient of $10^{-1}km^{-1}$ (corresponding to $\Gamma = 7.9 \times 10^{-10}cm^2J^{-1}$), the total fluence would be less than 6×10^6 J. This is really an upperlimit on the fluence, since here the inequality in eq. (51) has been taken to be an equality.

Finally let me emphasize some of the uncertainties of the present work. The growth rates given in equations (27), (30), (38), and (43) represent our best estimate of the perturbation growth rates in the simple model based on a uniform atmosphere. The approximations were based partly on physical grounds and are therefore not rigorous. In particular the effect of neglecting the integration around the branch cut, in interpretation of eq. (43) was not rigorously justified. Further, since the growth rate depends on the direction of $\underline{k}_\perp$, the quantity G may be large over a small range of angles. The question of how small that angle must be to avoid substantial degradation of the beam is not answered in the present work. Also, let me reemphasize that the borders between regimes in figures 3, 5, and 6 have been artificially smoothed. In conclusion, one should regard the growth rates obtained in this memo as indicative, and helpful in understanding the scaling of the instability and as a basis for understanding some of the complexities of the more exact numerical simulations.

Acknowledgements

The author wishes to acknowledge useful conversations with R. J. Briggs, M. Caplan, R. J. Hawkins, and E. T. Scharlemann.

References

[1] J. R. Morris (1987), "Unstable Growth of Perturbations in Thermal Blooming of Collimated Beams," Presentation at SDIO Workshop, Kirkland AFB, New Mexico, 15 Sep. 1987.

[2] J. F. Schonfeld, "Time Dependent Thermal Blooming/Turbulence Propagation Code: Design, Motivations, Requirements," Lincoln Laboratory, Lexington, Mass, BCP-3 (1987).

[3] T. J. Karr, "Status of Atmospheric Propagation Research," Presentation at the PCAP Meeting, Lincoln Laboratory, Lexington, Massachusetts, 21-22 April 1988.

[4] R. J. Briggs, Models of High Spatial Frequency Thermal Blooming Instabilities, Lawrence Livermore National Laboratory, Livermore, Calif., UCID-21118, (1987).

[5] A. J. Glass, "A Possible Strategy for Compensation of the Thermal Rayleigh Instability," 4 Aug 1987 (Draft).

[6] M. Rosenbluth, "Thermal Blooming in the Presence of Wind Shear," 3 Aug 1987 (Draft).
[7] F. W. Perkins, "Filamentation Instabilities", 3 Aug 1987, (Draft).
[8] T. J. Karr, Thermal Blooming Compensation Instabilities, Lawrence Livermore National Laboratory, Livermore, Calif., UCID 21172 (1987).
[9] J. J. Barnard, Fine Scale Thermal Blooming Instability: A Linear Stability Analysis, Appl. Optics, **28**, 438 (1989).
[10] K. A. Brueckner and S. Jorna, Phys. Rev. **164**, 182 (1967).
[11] V. V. Vorob'ev and V. V. Shemetov, Izv. Vyssh. Ucheb. Zaved. Radiofiz. **21**, 1610 (1978) [Sov. Phys. **33**, 1119 (1979)].
[12] J. Mathews and R. L. Walker, Mathematical Methods of Physics, (Benjamin/ Cummings; Menlo Park, California, 1964, Chap. 1)
[13] I. S. Gradshteyn and I. M. Ryzhik, Table of Integral, Series, and Products, (Academic Press; New York, 1980).
[14] R. J. Briggs,"Control of High Spatial Frequency Thermal Thermal Blooming Instabilities," Lawrence Livermore National Laboratory, March 1987 (Draft).
[15] V. Krapchev,"Atmospheric Effects on the Propagation of a High Energy FEL," presentation at Science Research Laboratory, Somerville, Massachusetts, March 23, 1988.

Figure Captions

1. The complex s_o plane for the integration of equation (23) in the large $k_\perp$ limit. All of the zeroes in eq. (41) lie along the dashed line. The branch of the logarithm in eq. (41) is chosen such that $-\pi < \theta < \pi$, where $\theta = \arg(1 + \frac{s_w}{s_o})$. The figure is drawn for $s_D = |s_w|$; larger values of $s_D/|s_w|$ result in more poles.
2. Schematic representation of phase compensated fine scale thermal blooming gain in the $\kappa - \tau$ plane. Asymptotic regimes and the respective gains for each region are shown. Dashed lines indicate contours of constant gain G where $I_1(h)/I_1(0) \sim \exp(G)$. The three contours shown are for G = 1, 3, and 10. Double dashed lines schematically indicate closely spaced contours due to the decay of the perturbations. The distortion number, $N_D = \Gamma I_0 k h t$, is held constant. The normalized variables are

$$\kappa = (h/2k)^{1/2} k_\perp, \quad \tau = (2k/h)^{1/2} c_s t, \quad x = (2k/h)^{1/2} \chi / c_s, \quad \text{and} \quad \lambda_\perp = 2\pi/k_\perp.$$

   For this figure the following parameters have been assumed: $N_D = 1000, h = 5 \times 10^5$ cm, $k = 6.3 \times 10^4$ cm^{-1}, $\chi = .22$ cm^2 s^{-1}, $\phi = \pi/2$, $c_s = 3 \times 10^4$ cm s^{-1}.
3. Surface plot of smoothed logarithmic gain. The approximate gain using the same parameters as in fig 2. In order to artificially smooth the sharp boundaries between regimes, the growth rate plotted is the inverse of the sum of inverse growth rates plus the decay rates.
4. Same as figure 2, except that $\phi = 0$, and $|d\underline{v}/dz| = v_o/h$, with $v_o = 450$ cm s^{-1}.
5. Same as figure 3, except that $\phi = 0$, and $|d\underline{v}/dz| = v_o/h$, with $v_o = 450$ cm s^{-1}.
6. Surface plot of smoothed logarithmic gain as a function of ϕ (the angle between the wind shear direction and $\underline{k}_\perp$) and $\log \kappa$. Here the parameters are the same as figure 2, except that $N_D = 150$, and $|d\underline{v}/dz| = v_o/h$, with $v_o = 450$ cm s^{-1}.

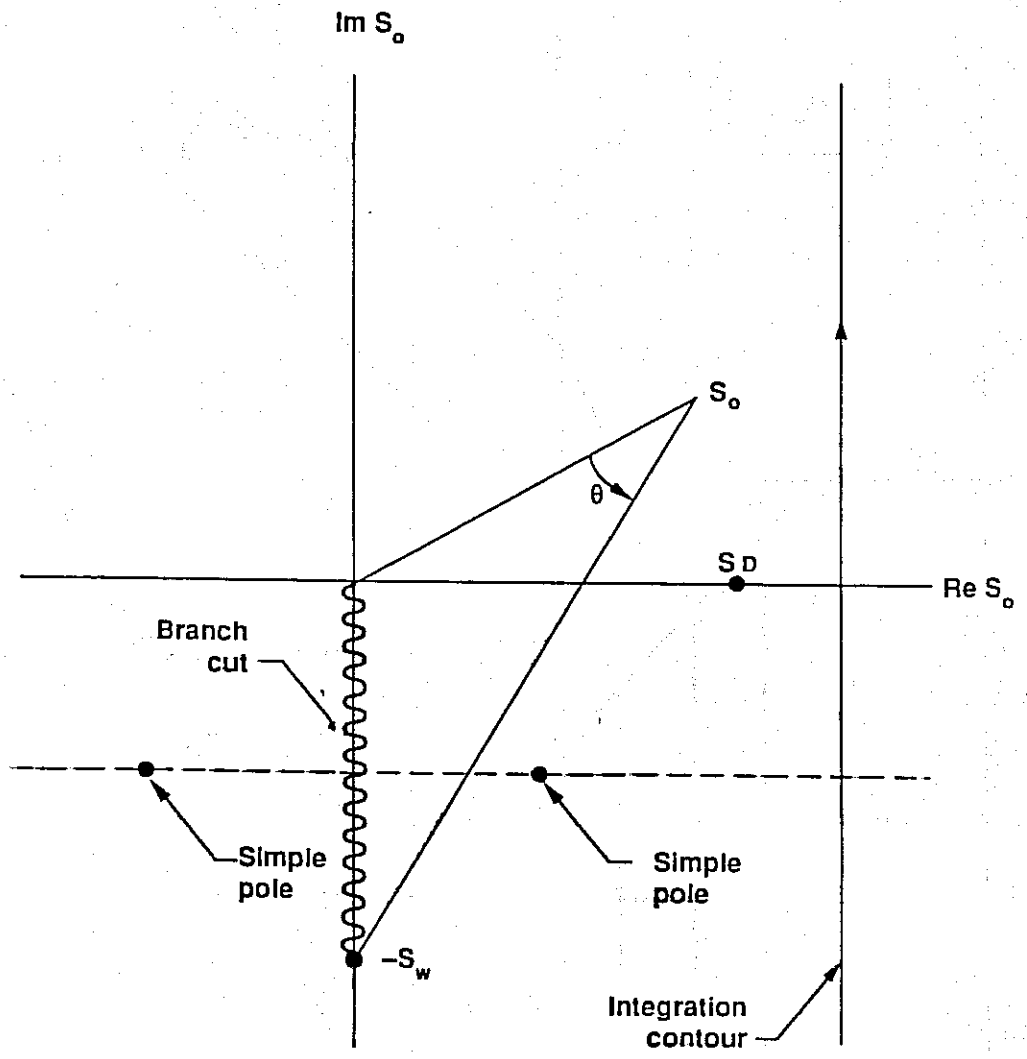
Im S_o
S_o
θ
S_D
Re S_o
Branch cut
Simple pole
Simple pole
$-S_w$
Integration contour

FIGURE 1

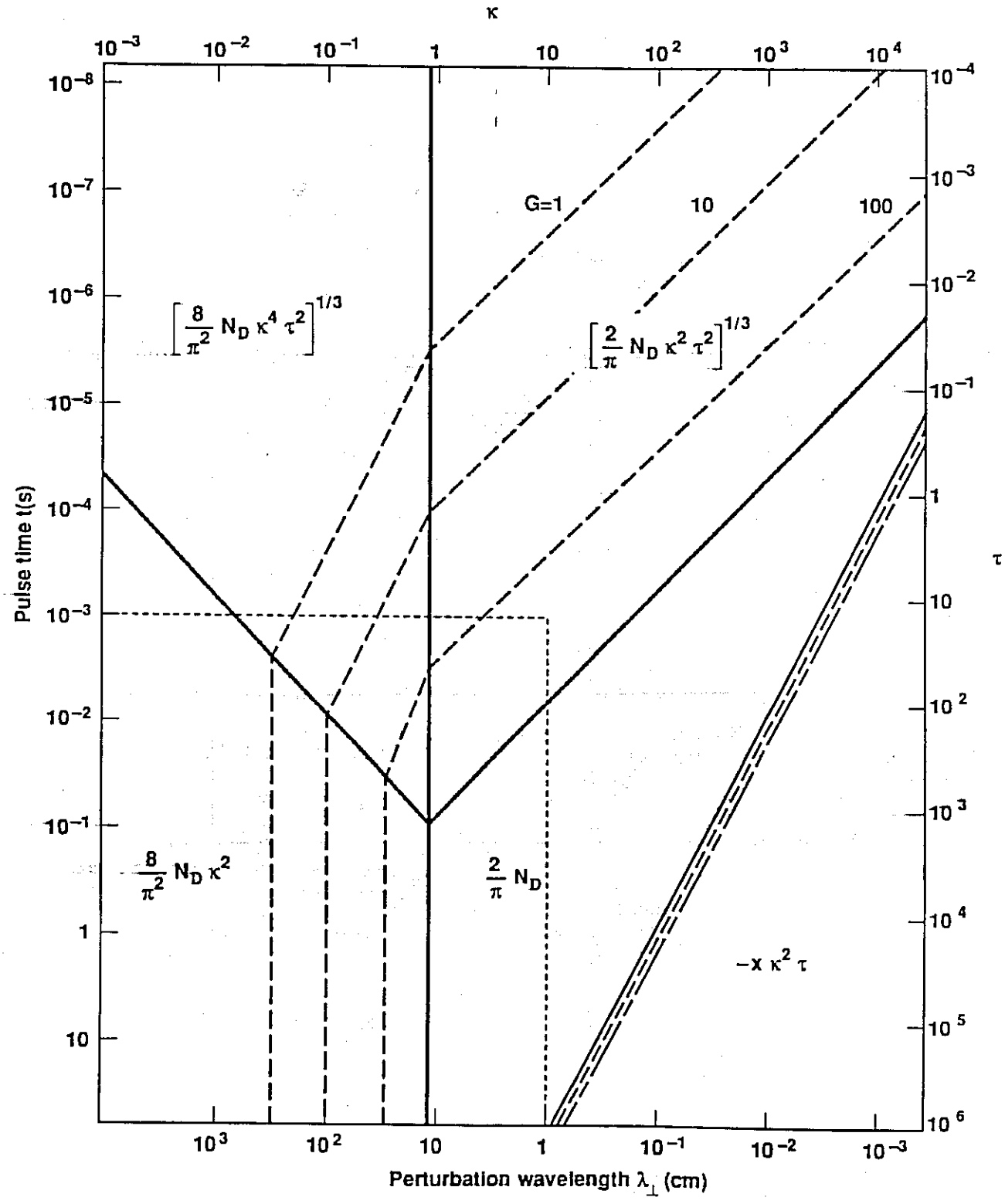

FL-020-U-8419-01

FIGURE 2

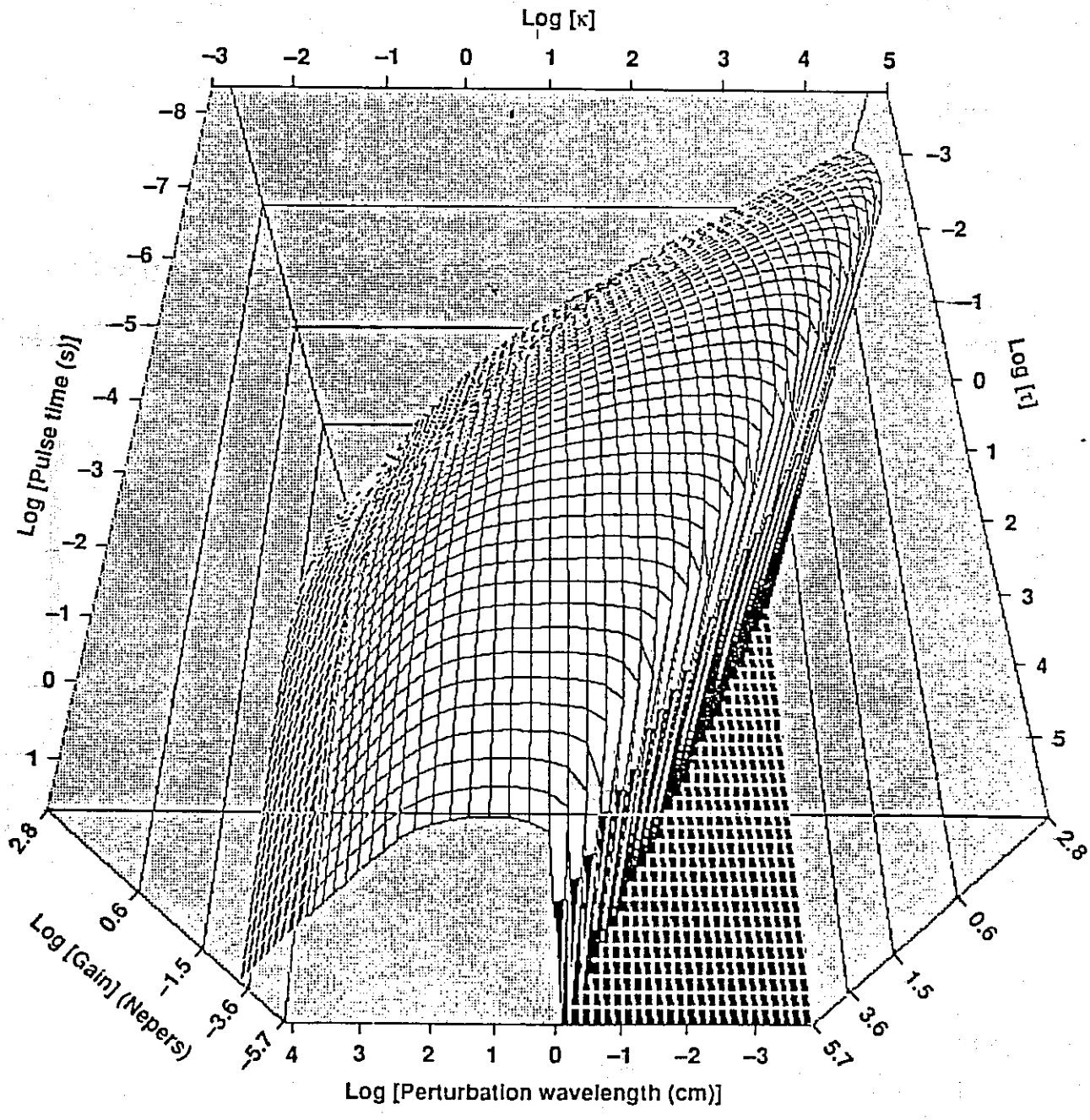
Log [κ]
−3 −2 −1 0 1 2 3 4 5
Log [Pulse time (s)]
−8 −7 −6 −5 −4 −3 −2 −1 0 1
Log [τ]
−3 −2 −1 0 1 2 3 4 5
Log [Gain] (Nepers)
2.8 0.6 −1.5 −3.6 −5.7
Log [Perturbation wavelength (cm)]
4 3 2 1 0 −1 −2 −3
2.8 0.6 1.5 3.6 5.7

FIGURE 3

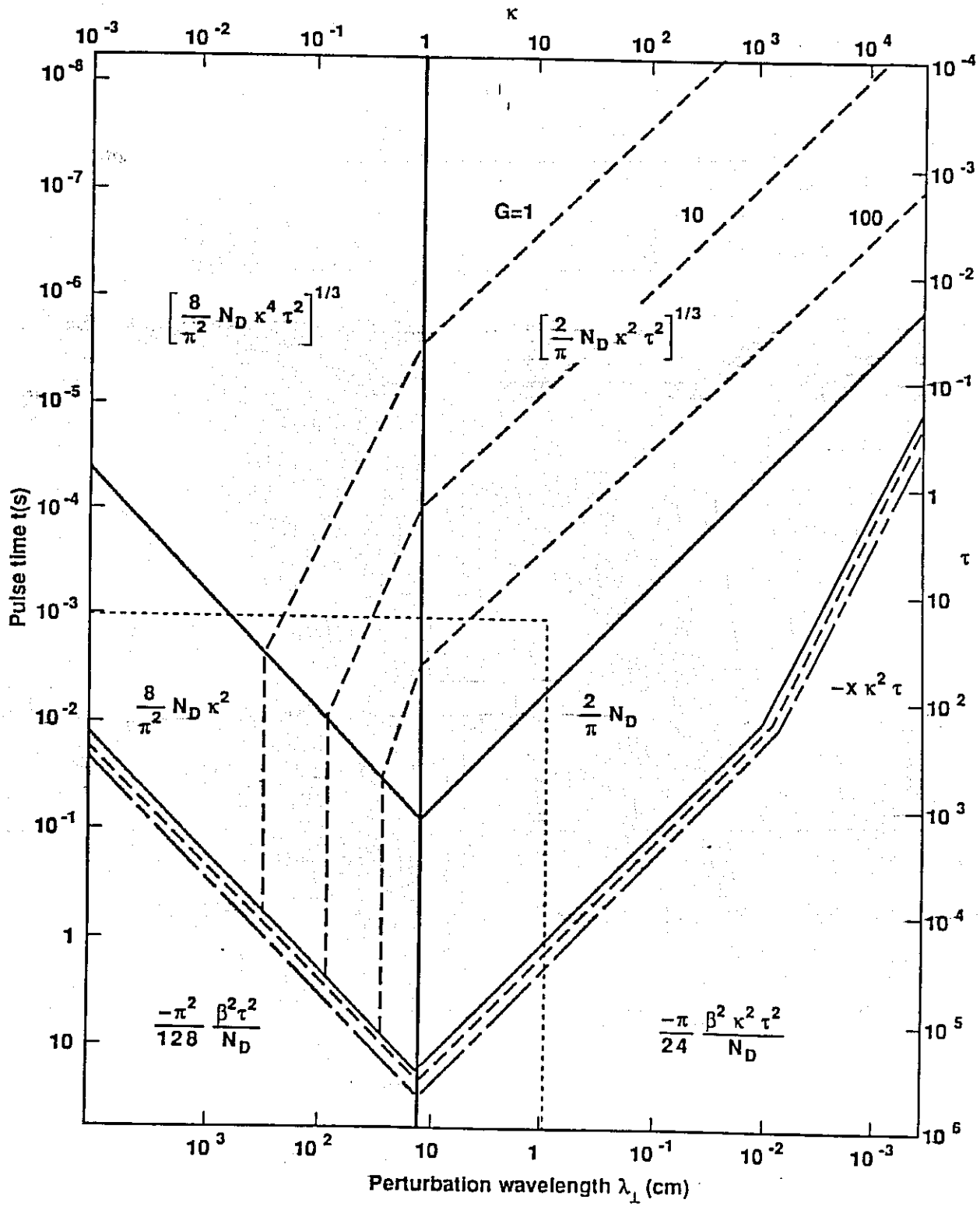

HK-004-U-8419-2-PM

FIGURE 4

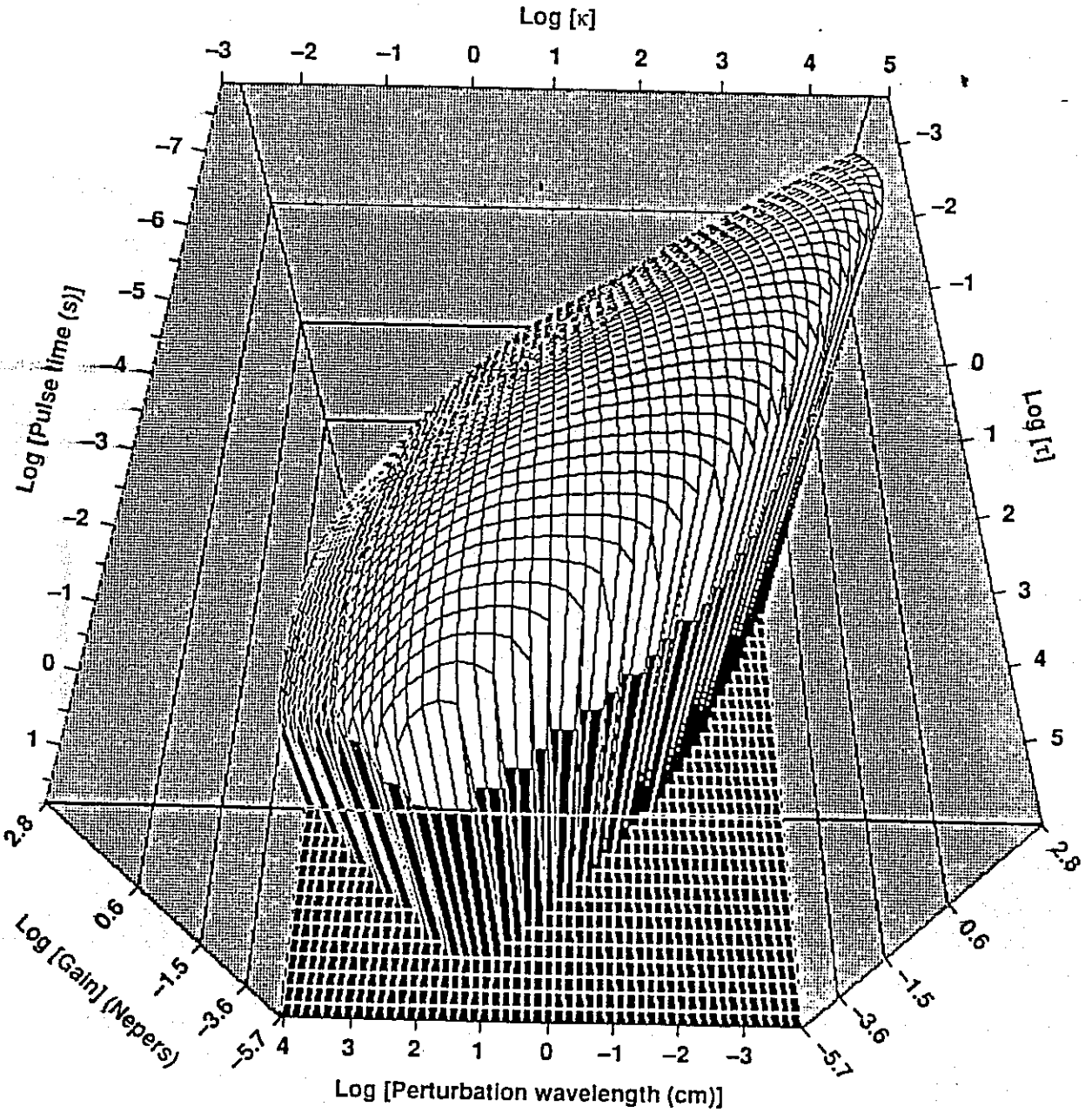
Log [κ]
−3 −2 −1 0 1 2 3 4 5
Log [Pulse time (s)]
−7 −6 −5 −4 −3 −2 −1 0 1
Log [τ]
−3 −2 −1 0 1 2 3 4 5
Log [Gain] (Nepers)
2.8 0.6 −1.5 −3.6 −5.7
4 3 2 1 0 −1 −2 −3
Log [Perturbation wavelength (cm)]

FIGURE 5

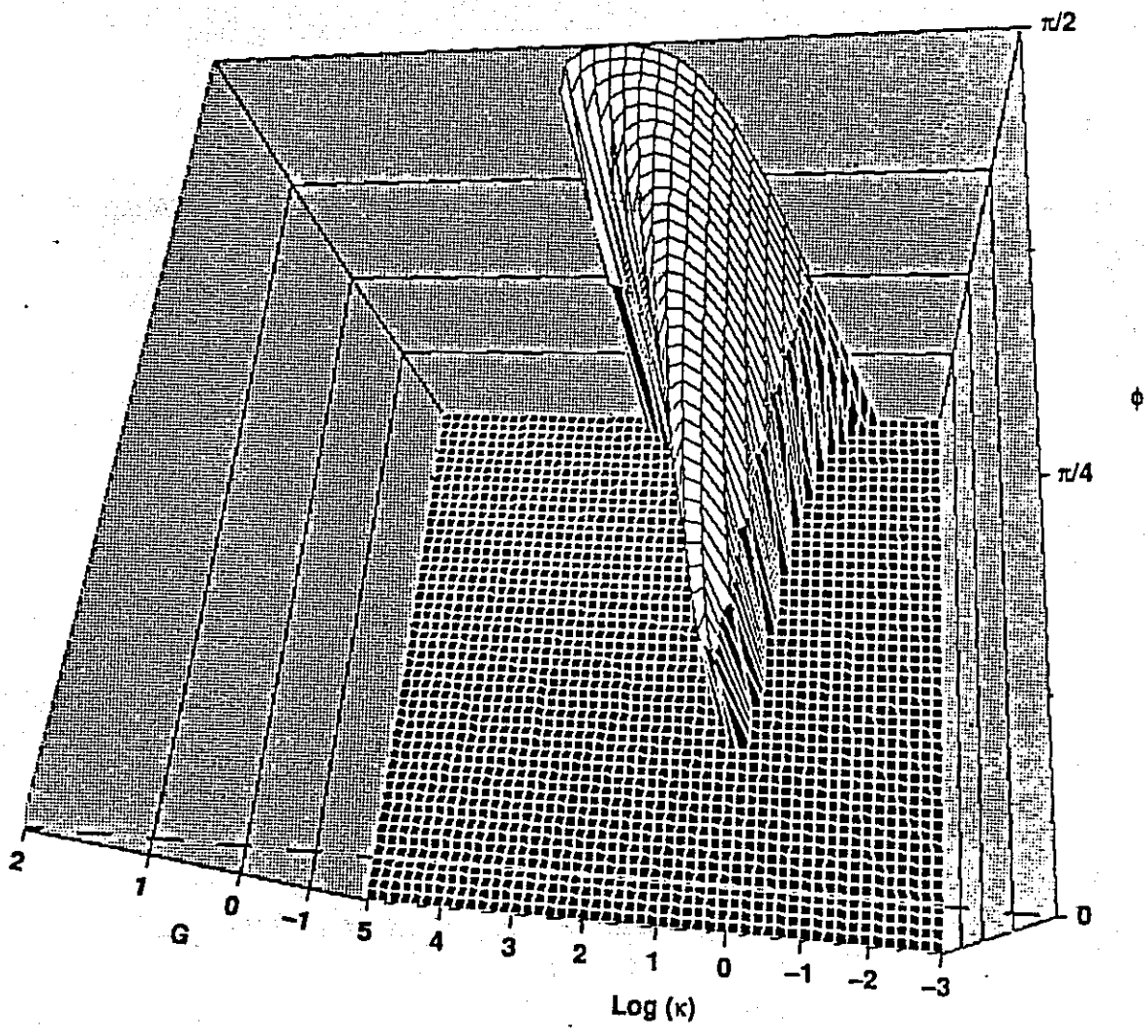

FIGURE 6